Zeitschrift: Bulletin des Schweizerischen Elektrotechnischen Vereins
Herausgeber: Schweizerischer Elektrotechnischer Verein ; Verband Schweizerischer Elektrizitätswerke
Band: 51 (1960)
Heft: 20

Artikel: Effect of Upper Side Bands in Travelling Wave Parametric Amplifiers
Autor: Dayem, A.
DOI: https://doi.org/10.5169/seals-917075

Effect of Upper Side Bands in Traveling Wave Parametric Amplifiers

By *A. Dayem*, Murray Hill

621.375.9.029.6

1. Introduction

The traveling wave type parametric amplifier has been analyzed by *Tien* and *Suhl* [1][1]) and others [2...6] who considered that the circuit carries only signal, idler, and pump frequencies. It has also been studied by *Roe* and *Boyd* [3] using a nondispersive infinitely wide-band transmission line. The effect of higher side bands on parametric amplification, however, is not fully understood.

In this paper parametric circuits containing a successively increasing number of upper side bands are studied. It will be shown that the parametric circuit is capable of four different types of behavior, or four different states, depending upon the number of side bands it carries. Thus, if the circuit carries $4n$—1 side bands, an exponentially growing mode which is synchronous with the pump wave is obtained. The 3-frequency case described previously [1—6] belongs to this group ($n=1$). Circuits which carry $4n$ side bands do not possess a growing mode but have, instead, a nongrowing synchronous mode in which only the even side bands are present. When the number of side bands is further increased by one, i.e. $4n+1$, gain becomes possible but the growing mode here has a sinusoidally varying amplitude. Finally, for circuits carrying $4n+2$ side bands there is a nongrowing synchronous mode in which only the odd side bands are present.

Excitation of the different modes of the circuit by an input at any side band frequency also is discussed. The growing mode, in particular, can be excited with an appreciable amplitude only if the input is at either the signal or the idler frequencies. Upper side bands are coupled weakly to the growing mode. Consequently the noise performance of the circuit does not deteriorate appreciably because of their presence.

In the last section of this paper the solution of the nondegenerate case is obtained for an infinitely wide-band parametric circuit. As in the degenerate case, power supplied by the pump to the system goes into increasing the side band amplitudes and no exponential gain is present.

2. Parametric Propagating Circuits of Limited Bandwidth

The equivalent circuit shown in Fig. 1 has been described by *Tien* and *Suhl* [1] and others [2...6]. It represents a uniform transmission line embedded in a medium having a nonlinear dielectric constant. When energized by a pump wave the line capacitance is assumed to be given by

$$C = C_0\left(1 + \frac{1}{2}\xi\, e^{j\theta} + \frac{1}{2}\xi\, e^{-j\theta}\right) \tag{1}$$

where

$$\theta = \omega t - \beta z \tag{2}$$

and ω and β are the frequency and the phase constant of the pump wave. The modulation constant ξ depends on the pump amplitude and the properties of the medium. A signal of frequency $\omega_1 = \alpha\omega$ is applied at the input. Its amplitude is assumed small compared to that of the pump so thet its effect on the line capacitance can be neglected. The propagation along the line can be described, therefore, by the equation

$$\frac{\partial^2 V}{\partial z^2} = L_0 \frac{\partial^2 (CV)}{\partial t^2} \tag{3}$$

where $V = V(z, t)$ is the voltage, L_0 and C_0 are the inductance and the unperturbed capacitance per unit length, and $\beta = \omega\sqrt{L_0 C_0}$

2.1 The infinite series solution

It is obvious that the solution of Eq. (3) should contain all side bands of frequencies $n\omega \pm m\omega_1$. However, the signal may be assumed small enough compared with the pump so that the side bands $\omega \pm m\omega_1$ with $m>1$, resulting from multiple mixing with the signal, can be neglected. Hence one may write the solution of Eq. (3) in the form

$$V(z, t) = \sum_{n=-\infty}^{\infty} (V_n(z)\, e^{j(n-\alpha)\theta} + \text{c.c.}) \tag{4}$$

assuming that the line is perfectly terminated at all frequencies. (c. c. means complex conjugate.) Substituting Eqns. (4) and (1) in Eq. (3) and equating terms of equal frequencies, one obtains

$$\frac{d^2 V_n}{dz^2} - 2j(n-\alpha)\beta\frac{dV_n}{dz} = -\frac{1}{2}\xi(n-\alpha)^2\beta^2(V_{n-1} + V_{n+1}) \tag{5}$$

$$\text{for } -\infty < n < \infty$$

The complex conjugate of Eq. (5) holds for V_n*. Since we are primarily interested in growing modes which generally satisfy the condition that $\left|\frac{dV_n}{dz}\right| \ll |\beta V|$, the second derivative in Eq. (5) may be neglected and we get a double infinite set of differential equations of the first order, namely

$$\frac{dV_n}{d\gamma} = -j\frac{1}{4}\xi\beta(n-\alpha)(V_{n-1} + V_{n+1}) \tag{6}$$

$$\text{for } -\infty < n < \infty$$

This set possesses solutions of the form $\exp\left(\frac{1}{4}\xi\beta\zeta z\right)$, which reduce it to the double infinite set of algebraic equations

$$\zeta V_n = -j(n-\alpha)(V_{n-1} + V_{n+1}) \tag{7}$$

$$\text{for } -\infty < n < \infty.$$

For any finite range of n equations Eq. (7) can be solved for ζ and the corresponding amplitudes.

2.2 Four different states for a parametric circuit

The wave solution Eq. (4) contains an infinite number of side bands. In a practical circuit, however, dispersion and cutoff characteristics may limit the number of side bands which contribute to the parametric interaction. An adequate description of the practical case may be obtained by con-

[1]) Refer to the Bibliography at the end of the article.

sidering an idealized low-pass filter which possesses no dispersion at any frequency lower than its cutoff frequency ω_c. Such a filter may be represented by Eq. (7) if all side bands of frequencies greater than ω_c are neglected. This leads to the finite set of equations

$$\begin{aligned} \zeta V_{-M} - \mathrm{j}(M+\alpha) V_{-M+1} &= 0 \\ \zeta V_n + \mathrm{j}(n-\alpha)(V_{n-1} + V_{n+1}) &= 0 \quad -M+1 \leqq n \leqq N-1 \\ \zeta V_N + \mathrm{j}(N-\alpha) V_{N-1} &= 0 \end{aligned} \tag{8}$$

Here M and N are positive integers given successively by one of the following pairs of values:

1. the 3-f case with $M = 0, N = 1$
2. the 4-f case with $M = 0, N = 2$
3. the 5-f case with $M = 1, N = 2 \ldots$ etc.

The phrase "n-f case" denotes the case where n side bands (including pump, signal, and idler) lie within the pass band of the circuit.

The set of homogeneous equations (8) have nontrivial solutions if the determinant of the coefficients vanishes. This leads to a characteristic equation of the form

$$\zeta^K + A_1 \zeta^{K-2} + \ldots + A_L \zeta^{K-2L} + \ldots + A_{K/2} = 0 \tag{9}$$

when $K = M + N + 1$ is even, and

$$\zeta \left\{ \zeta^{K-1} + A_1 \zeta^{K-3} + \ldots + A_L \zeta^{K-2L-1} + \ldots + A_{(K-1)/2} \right\} = 0 \tag{9a}$$

when K is odd. The coefficients A are all real and can be expressed in the general form

$$\begin{aligned} A_L = & \sum_{n_1=-M}^{N_1} (n_1 - \alpha)(n_1 - \alpha + 1) \ldots \\ & \sum_{n_2=n_1+2}^{N_1+2} (n_2 - \alpha)(n_2 - \alpha + 1) \ldots \\ & \sum_{n_L=n_{L-1}+2}^{N-1} (n_L - \alpha)(n_L - \alpha + 1) \end{aligned} \tag{10}$$

where $N_1 = N - 2L + 1$.

First apply Descartes' rule of signs [7] to determine whether the characteristic equation has any real positive roots. A detailed study of Eq. (10) shows that A_L is always positive for all values of $L \neq \frac{k}{2}$. The coefficient $A_{K/2}$ is negative when $M = 2p$ and $N = 2p + 1$ ($p = 0,1,2,\ldots$) and is positive otherwise. From Descartes' rule it follows that Eq. (9a) has no real positive roots for any values of M and N while Eq. (9) has *one* real positive root, if

$$M = 2p \text{ and } N = 2p + 1 \tag{11}$$

This result is in agreement with the well-known fact that exponential gain is possible in a parametric circuit which carries only signal, idler, and pump frequencies. This 3-f case is obtained from Eq. (11) for $p = 0$. The next case which possesses a similar growing mode is the 7-f case corresponding to $p = 1$ in Eq. (11). Thus, the same behavior repeats itself when four more side bands are added. However, the addition of one more side band to any of the cases represented by Eq. (11) leads us to those given by

$$M = 2p, N = 2p + 2 \tag{12}$$

Here the characteristic equation is given by Eq. (9a) which possesses no real positive roots and thus a different type of behavior is obtained. Eq. (9a) also represents those cases given by

$$M = 2p + 1 \text{ and } N = 2p + 3 \tag{13}$$

which contain three more side bands than the cases given by Eq. (11) for the same values of p. It is to be noted that Eq. (9a) has a zero root which, if substituted in Eq. (8), gives

$$V_n = 0 \text{ for } \textit{odd} \text{ values of } n \tag{14}$$

for those cases given by Eq. (12), and

$$V_n = 0 \text{ for } \textit{even} \text{ values of } n \tag{15}$$

for those given by Eq. (13). No further information is directly available from the characteristic equation and one has to resort to numerical methods to determine the nature of the other modes of the circuit.

The numerical solution of equations (9) and (9a) gives the following two results:

1. Eq. (9) has 2 pairs of complex conjugate roots for cases satisfying
$$M = 2p + 1 \text{ and } N = 2p + 2. \tag{16}$$
2. All remaining roots of either Eq. (9) or (9a) occur as purely imaginary conjugate pairs.

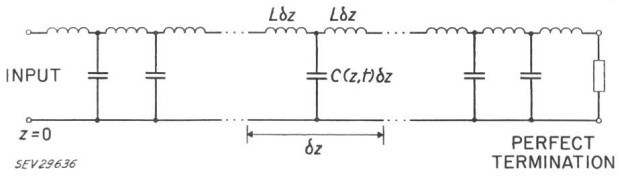

Fig. 1
Distributed parametric circuit

The above discussion clearly demonstrates that the parametric circuit is capable of four different types of behavior which repeat themselves sequentially as the number of side bands is increased. For ease of future reference we may identify them by the following four "states":

State 1 $(M = 2p, N = 2p + 1)$:

includes the 3-f, 7-f, and 11-f, ... cases and possesses a growing and a decaying mode varying as $e^{\pm\delta\varphi}$, where δ is real positive and

$$\varphi = \frac{1}{4} \xi \beta z \tag{17}$$

Both modes are synchronous with the pump wave.

State 2 $(M = 2p, N = 2p + 2)$:

includes the 4-f, 8-f, 12-f, ... cases and possesses a constant amplitude synchronous mode satisfying Eq. (14).

State 3 $(M = 2p + 1, N = 2p + 2)$:

includes the 5-f, 9-f, 13-f, ... cases. It possesses two growing modes varying as

$$e^{\delta\varphi \pm \mathrm{j}\gamma\varphi}$$

i.e. one slower and the other faster than the pump. They may be combined in a growing wave of periodically varying amplitude of the form

$$e^{\delta\varphi} \cos \gamma\varphi$$

State *3* obviously possesses the corresponding decaying modes

$$e^{-\delta\varphi \pm j\gamma\varphi}$$

State 4 ($M = 2p + 1, N = 2p + 3$):

includes the 6-*f*, 10-*f*, 14-*f*, ... cases and possesses a constant amplitude synchronous mode satisfying Eq. (15).

In addition to the modes mentioned above, the parametric circuit possesses propagating modes which occur in pairs and vary like exp ($\pm j\gamma_i\varphi$), i.e. one faster and the other slower than pump. Each pair can be combined in a wave of periodically varying amplitude.

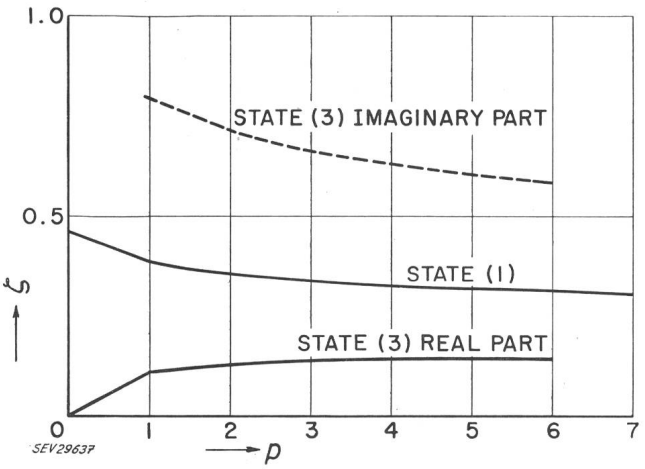

Fig. 2

ζ vs. p for the growing modes with $\alpha = 0.7$

The real root of State *1* and the complex root of State *3* are shown in Fig. 2 as a function of p. It is seen that the gain decreases in State *1* and increases in State *3* with increasing p, i.e. as the number of side bands carried by the circuit is

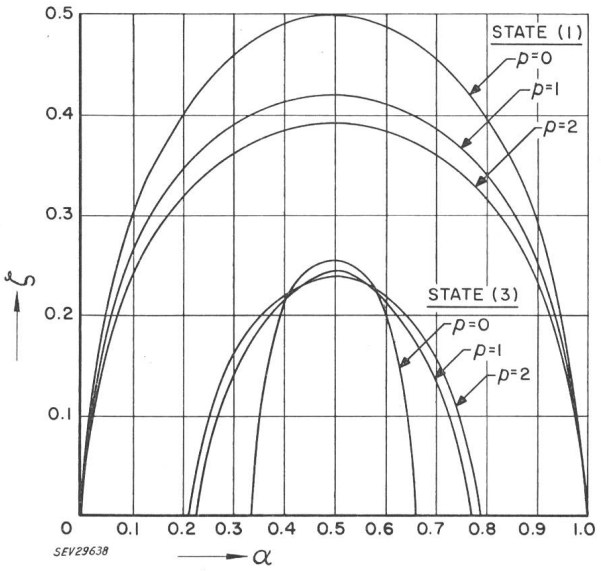

Fig. 3

ζ vs. α for the growing modes

increased. Fig. 3 shows the same roots as functions of α. The maximum gain in either state is achieved when $\alpha = 1/2$. We notice also that the gain in State *3* does not extend over the whole range of α.

The imaginary roots show an interesting pattern when plotted against p as in Fig. 4. Notice that the roots starting at $p = p_1$ decrease with slowing rate for $p > p_1$. However, it is evident from Fig. 2 and 4 that the convergence of the series solution is rather slow and no conclusions can be drawn about the behavior as $p \to \infty$.

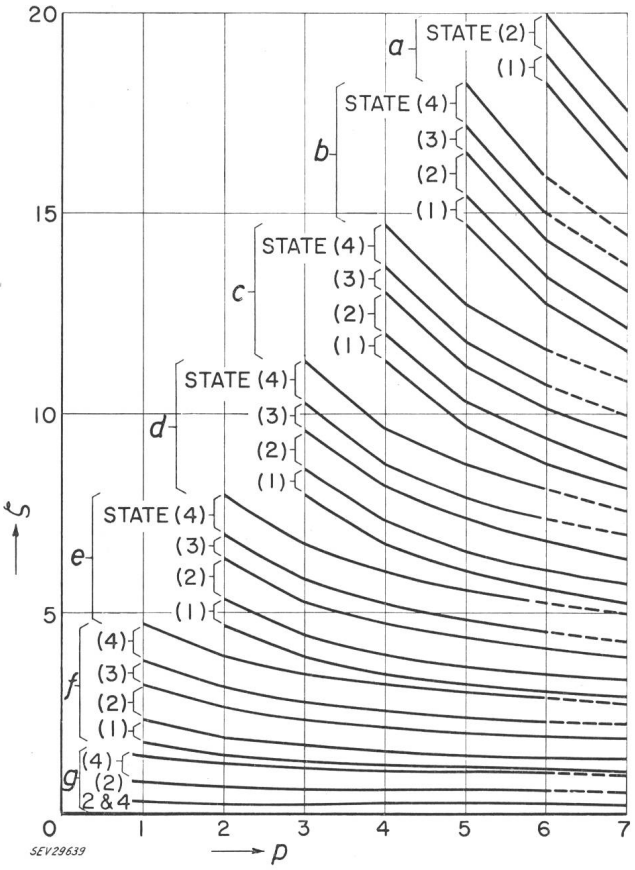

Fig. 4

Imaginary roots for the four states with $\alpha = 0.7$

2.3 Relative amplitudes

Denote the K roots of the characteristic equation by $\zeta_1, \zeta_2, \ldots, \zeta_K$. Each root defines a possible mode of the parametric circuit. Each mode, in turn, is composed of a specific linear combination of the K side bands considered. The relative amplitudes of these side bands are determined for the i th mode by substituting ζ_i in Eq. (8) and solving for

$$a_{ni} = \frac{V_{ni}}{V_{oi}} \qquad (18)$$

with $a_{oi} = 1$

Here the first subscript refers to the side band frequency and the second refers to the mode.

Two examples of the relative amplitudes are shown in Fig. 5 and 6. They belong to the growing mode of State *1* for $\alpha = 0.3$ and $\alpha = 0.7$ respectively. One observes that the amplitude distributions in Fig. 5 and 6 are not identical although the corresponding values of α indicate identical side band frequencies and identical modes. The explanation of this difference can be seen easily from Eq. (8). It suffices here to remark that the two distributions would be identical if the roles of signal and idler were interchanged. It can be

seen that some of the upper side bands have amplitudes greater than the signal amplitude. In fact, one may gain 4 db if the output is taken at any side band of frequency $(2n + 1)\omega - \omega_1$ rather than at the signal. Thus the growing mode of State *1* also may be used with advantage as a frequency up-converter.

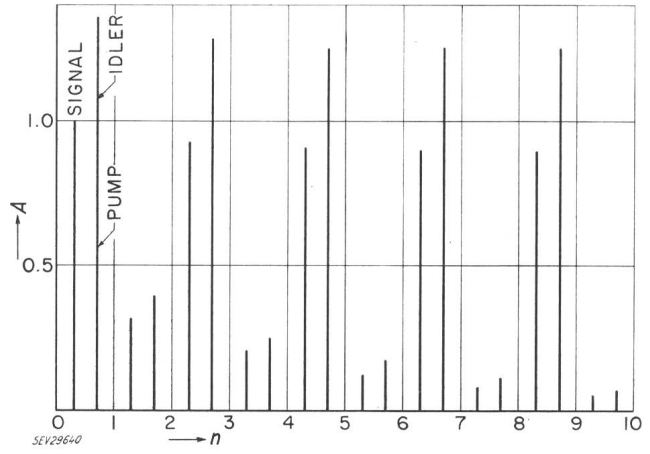

Fig. 5

Relative amplitudes of the growing mode in state *1* with $\alpha = 0.3$

Similar relative amplitude distributions are obtained for the other modes of all the states. For the sake of brevity they will not be included in this paper.

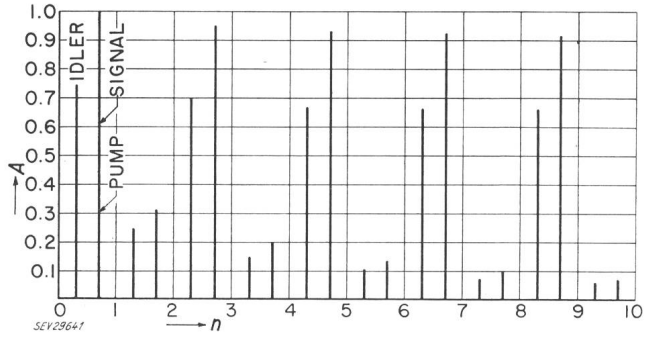

Fig. 6

Relative amplitudes of the growing mode in state *1* with $\alpha = 0.7$

2.4 Boundary conditions and excitation of different modes

The complete solution describing the behavior of a parametric circuit can be written as a linear combination of all the possible modes. Using Eqns. (4) and (18) one gets

$$V(z,t) = \sum_{i=1}^{k} U_i \, e^{\zeta_i \varphi} \sum_{n=-M}^{N} a_{ni} \, e^{j(n-\alpha)\theta} + \text{c. c.} \quad (19)$$

The mode amplitudes U_i are constants to be determined from the boundary condition.

Let the boundary conditions be defined at $z = 0$ by the equation

$$V(O,t) = \sum_{n=-M}^{N} P_n \, e^{j(n-\alpha)\omega t} + \text{c. c.} \quad (20)$$

Putting $z = 0$ in Eq. (19) and equating it with Eq. (20), one obtains the K boundary equations

$$P_n = \sum_{i=1}^{k} a_{ni} \, U_i \qquad \text{for } -M \leqq n \leqq N \quad (21)$$

as well as the complex conjugate set of Eq. (21). It is obvious that either set is sufficient for determining the K complex unknowns U_i.

We wish here to emphasize that throughout this analysis the complex notation has been used to denote real quantities. The roots obtained turned out in general as imaginary conjugate pairs. Reference to Eqns. (8) and (18) shows that the relative amplitudes corresponding to one root are, except for a difference in sign, identical with those of the conjugate root. The same holds for the real positive and negative roots of State *1*. Similarly, the amplitudes U_i and U_{i+1} of a pair of conjugate modes are identical except for a sign difference. Thus, in the following discussion one may use U_{2i+1} to describe a pair of modes corresponding to the pair of roots ζ_{2i+1} and ζ_{2i+2}.

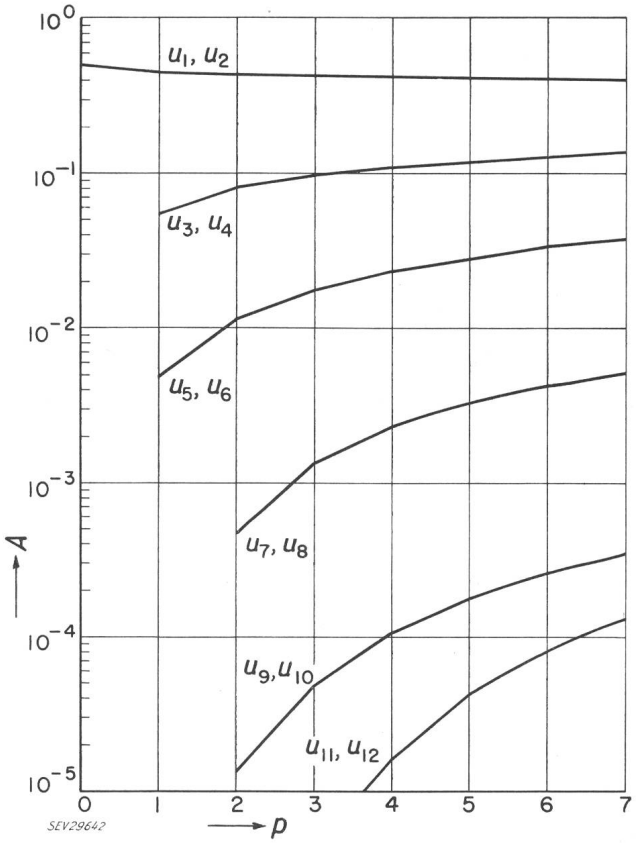

Fig. 7

Mode amplitudes A vs. p for state *1* with $\alpha = 0.3$

The first point of interest in this section is to find the degree of excitation of each mode by an input at the signal frequency only. In other words, one wishes to find U_i which satisfy the input condition

$$1 = \sum_{i=1}^{k} U_i$$
$$0 = \sum_{i=1}^{k} a_{ni} \, U_i \text{ for } n \neq 0 \quad (22)$$

The results for State *1* are summarized in Fig. 7, which shows the mode amplitudes against p for $\alpha = 0.3$. At $p = 0$ (the 3—f case) only the growing and decaying modes are present and each has an amplitude equal to one-half. One finds that U_1 gradually decreases as p is increased, and reaches a value of 0.4 at $p = 7$. Thus the addition of 24 upper side bands which give rise to 24 additional modes has resulted in a slight decrease in U_1 (less than 2 db). It is obvious from Fig. 7 that all the other modes possess very small amplitudes (10 db or more below U_1) when excited by an input at signal frequency. It may be concluded that the presence of the upper side bands and their associating modes has little effect on the behavior of State *1* as a parametric amplifier.

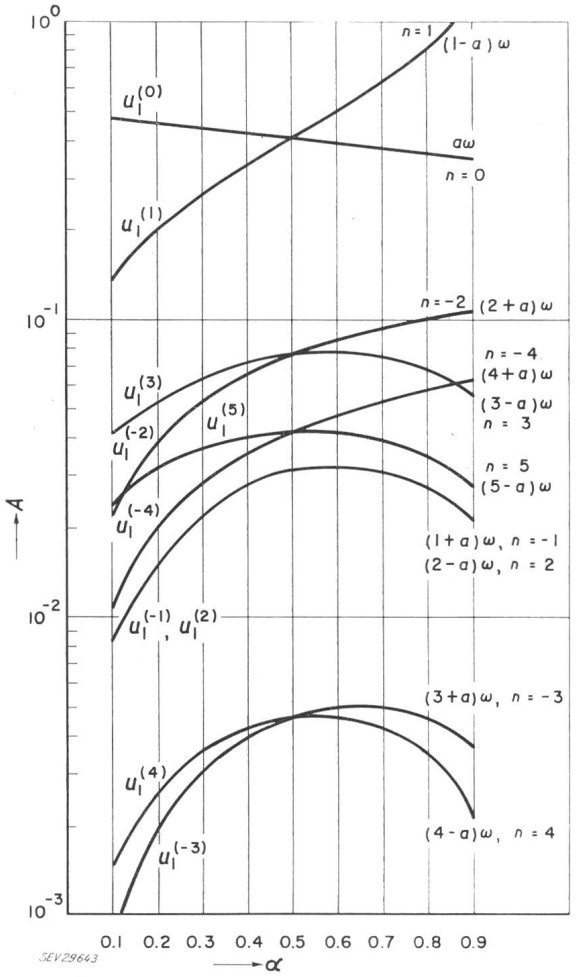

Fig. 8

Amplitudes of the growing mode $U_1^{(n)}$ excited by input at frequency $|n - \alpha|\,\omega$

The above remarks point out an important fact which has been verified by the numerical computations. If one adds one more side band a new mode is produced and the properties of the old modes will be modified slightly. Input power at the frequency of the newly added side band will go mainly into exciting the new mode. Only a small fraction of this input power will go into exciting the old modes. This fact will prove to be quite important in determining the noise behavior of the parametric amplifier.

The second point of interest in this section is the degree of excitation of the growing mode due to an input at any of the side band frequencies. Thus, we wish to find $U_1^{(r)}$ produced by an input at a frequency $(r - \alpha)\omega$, i.e., which satisfied the input equations

$$1 = \sum_{i=1}^{k} a_{ri}\, U_i^{(r)}$$
$$0 = \sum_{i=1}^{k} a_{ni}\, U_i^{(r)}, \qquad \text{for } n \neq r \tag{23}$$

The results are shown in Fig. 8. It is seen that the growing mode acquires a very small amplitude when excited by any upper side band. Further, it is noticed that the idler excites the growing mode with an amplitude slightly lower or slightly higher than that due to the signal depending on whether the idler frequency is higher or lower than the signal frequency. The growing mode amplitude excited by the signal decreases as the signal frequency increases. These remarks will be referred to later when discussing the noise figure.

2.5 Noise Considerations

Since the growing mode will predominate a short distance away from the input plane, one may neglect all the other modes of the circuit when calculating the amplifier noise figure. Thus, an input at a frequency $(r-\alpha)\,\omega$ will excite the growing mode with an amplitude $U_1^{(r)}$ which can be

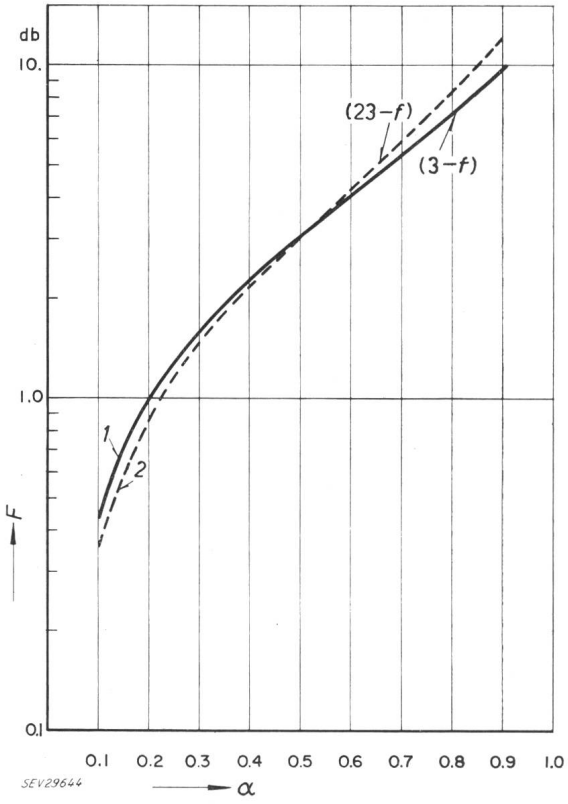

Fig. 9

Signal noise figure F vs. α

obtained from Eq. (23). Assuming that each side band contains the same amount of noise power at the input plane, the noise figure at the signal frequency is given by

$$F = \frac{\sum_{r=-M}^{N} |\, U_1^{(r)} \,|^2}{|\, U_1^{(0)} \,|^2} \tag{24}$$

Similarly, the noise figure at a frequency $(n - \alpha)\omega$ is

$$F^{(n)} = \frac{\sum_{r=-M}^{N} |a_{n1} U_1{}^{(r)}|^2}{|a_{n1} U_1{}^{(n)}|^2} = \frac{\sum_{r=-M}^{N} |U_1{}^{(r)}|^2}{|U_1{}^{(n)}|^2} \tag{25}$$

The signal to noise figure F plotted against α is shown in Fig. 9 where the solid curve is for the 3-f case (where $F = 1 + \omega_1/\omega_2$) and the dashed curve is for the 23-f case. For any intermediate case the noise figure curve will lie in the space between the solid and dashed curves. We observe immediately that the addition of 20 higher side bands produces but a small change in the noise figure. The noise figures of the individual side bands are shown in Fig. 10. As expected, the idler noise figure is of the same magnitude as that of the signal while the noise figures of the upper side bands are of higher order.

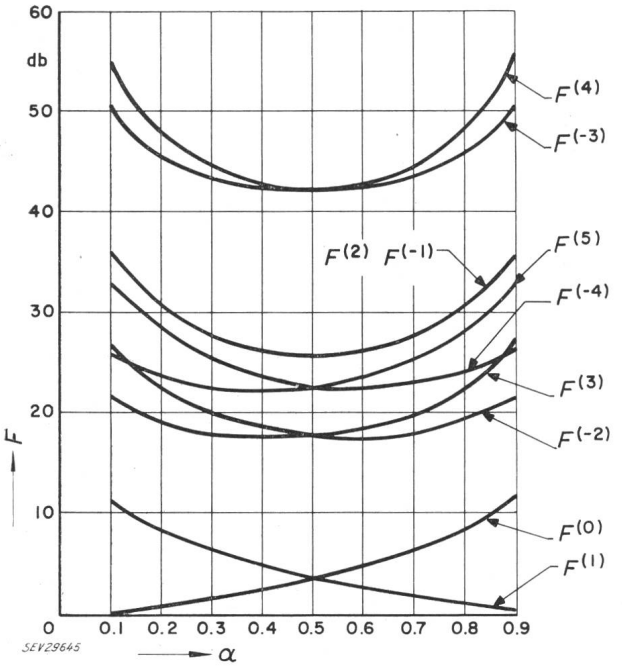

Fig. 10

Noise figures $F^{(n)}$ at frequency $|n - \alpha|\,\omega$

The noise behavior shown in Fig. 9 and 10 is explained easily by the facts discussed in the previous section. It was pointed out that an input power at either the signal or idler frequencies will go mainly into exciting the growing mode even when the circuit possesses a great number of modes. On the other hand, the growing mode receives only a small portion of the input power if the excitation is at an upper side band frequency.

3. Propagating Circuits of Infinite Band-Width

It was pointed out in Section 2 that the infinite series solution cannot be used to describe the behavior when the circuit band-width becomes infinite. An alternative method has been described by *Roe* and *Boyd* [3] and applied to the degenerate case where $\alpha = 1/2$. In this section the same method will be extended to the nondegenerate case.

Let the voltage be expanded in powers of ξ in the form

$$V = F(x, \theta) + \xi H(x, \theta) + \ldots \tag{26}$$

where

$$\theta = \omega t - \beta z \text{ and } x = \xi \beta z \tag{27}$$

Assuming the capacitance to be given by

$$C = C_0 (1 + \xi \sin \theta) \tag{28}$$

the wave equation (3) in terms of the new variables gives

$$\frac{\partial}{\partial \theta}\left[\frac{\partial}{\partial \theta}(F \sin\theta) + 2\frac{\partial F}{\partial x}\right] = 0 \tag{29}$$

and

$$\frac{\partial}{\partial \theta}\left[\frac{\partial}{\partial \theta}(H \sin\theta) + 2\frac{\partial H}{\partial x}\right] = \frac{\partial^2 F}{\partial x^2} \tag{30}$$

The solution of (29), subject to the initial condition

$$F(0,\theta) = \sin \alpha\theta \tag{31}$$

is found to be

$$F(x, \theta) = \frac{\sin \alpha T}{\cosh \frac{x}{2} + \sinh \frac{x}{2} \cos\theta} \tag{32}$$

where $T(x, \theta)$ is given by

$$\tan \frac{T}{2} = e^{-\frac{x}{2}} \tan \frac{\theta}{2} \tag{33}$$

Equations (32) and (33), combined for $\alpha = 1/2$ will give equation (9) in reference [5]. Since all the interesting information is contained in the leading function F [3], the solution of Eq. (30) will not be considered here.

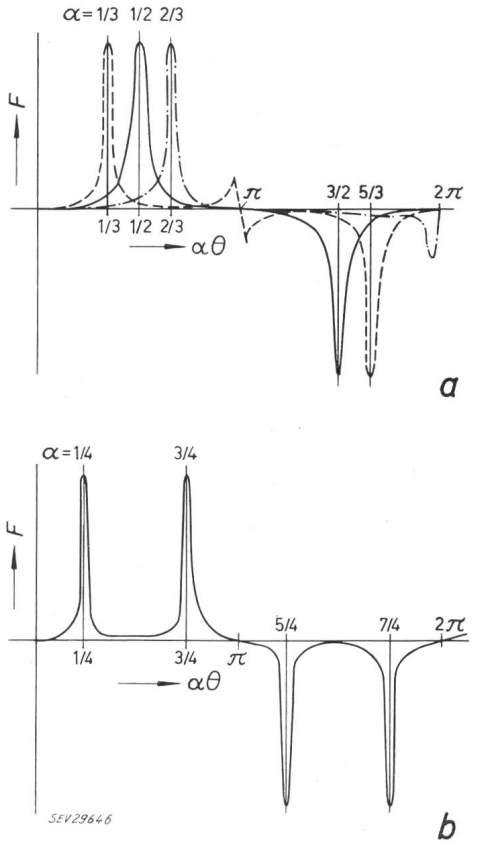

Fig. 11

Voltage at large values of x

The function F is plotted against $\alpha\theta$ in Fig. 11a and 11b for large x and different values of α. One finds that the sinusoidal input voltage of Eq. (31) is transformed at large values of z into a train of sharp pulses. These pulses occur when θ is an odd multiple of π, i.e., one pulse per pump

cycle independently of the value of α. It is interesting to note that such a circuit may be used to produce a train of pulses of very small width and high repetition rate and the pulses may be position modulated by frequency modulating the pump.

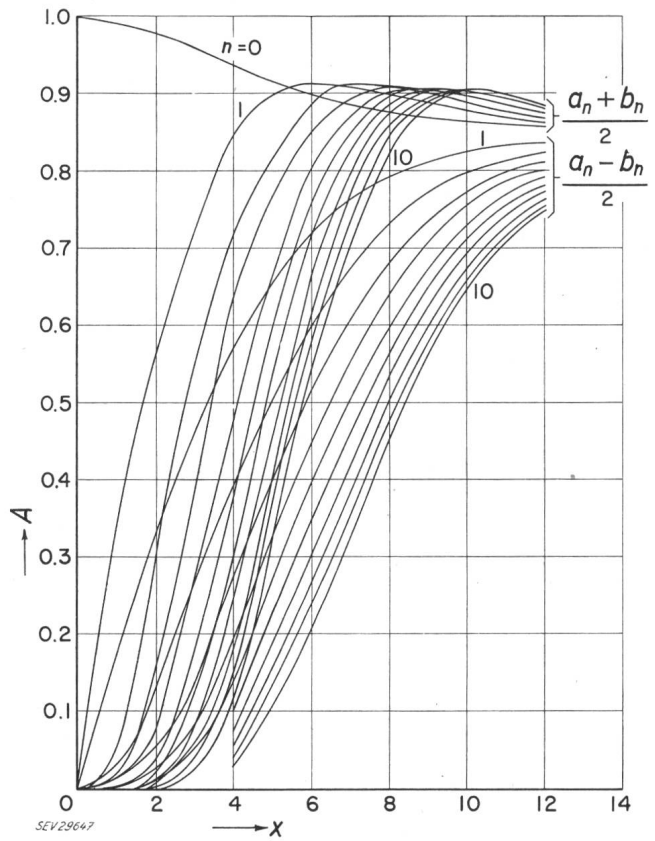

Fig. 12

Harmonic content A vs. x for $\alpha = 0.3$

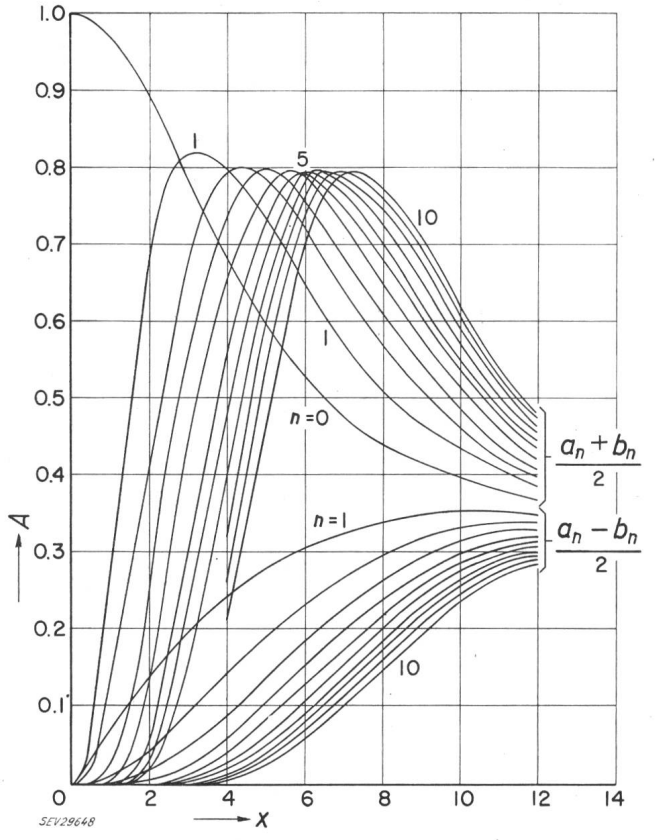

Fig. 13

Harmonic content A vs. n for $\alpha = 0.7$

To get the harmonic content of F, put $T = \theta + \varphi$ in (32) and (33) to get

$$F = \sin \alpha\theta(\mathrm{G}(x, \theta') \cos \alpha\varphi) + \cos \alpha\theta(\mathrm{G}(x, \theta') \sin \alpha\varphi) \quad (32a)$$

and

$$\tan \frac{\varphi}{2} = \frac{(1 - \mathrm{e}^{-x/2}) \sin \theta'}{(1 + \mathrm{e}^{-x/2}) - (1 - \mathrm{e}^{-x/2}) \cos \theta'} \quad (33a)$$

where $\theta' = \theta - \pi$ and

$$\mathrm{G}(x, \theta') = \left(\cosh \frac{x}{2} - \sinh \frac{x}{2} \cos \theta'\right)^{-1}$$

In Eq. (32a) $\sin \alpha\theta$ is multiplying an even function of θ' while $\cos \alpha\theta$ is multiplying an odd function. Thus the Fourier expansion of F can be written in the form

$$f = \sin \alpha\theta \sum_0^\infty a_n \cos n\theta' + \cos \alpha\theta \sum_0^\infty b_n \sin n\theta' =$$

$$= \sum_0^\infty (-1)^n \left[\frac{b_n + a_n}{2} \sin (n + \alpha)\theta + \frac{b_n - a_n}{2} \sin (n - \alpha)\theta\right] \quad (32b)$$

where

$$a_0 = \frac{1}{\pi} \int_0^\pi \mathrm{G}(x, \theta') \cos \alpha\varphi \, \mathrm{d}\theta'$$

$$a_n = \frac{2}{\pi} \int_0^\pi \mathrm{G}(x, \theta') \cos n\theta' \cos \alpha\varphi \, \mathrm{d}\theta' \quad (34)$$

$$b_n = \frac{2}{\pi} \int_0^\pi \mathrm{G}(x, \theta') \sin n\theta' \sin \alpha\varphi \, \mathrm{d}\theta'$$

It is worthwhile noting that F contains only components of frequencies $(n \pm \alpha)\omega$ which makes it similar in form to the infinite series solution expressed in equation (4). It is to be expected that the function H as well as the higher order terms in the expansion (26) will contain components of frequencies $(n \pm m\alpha)\omega$. Although these functions might contribute small corrections to the terms included in (32b), it seems that no important information is lost if they are neglected.

The amplitudes $(b_n + a_n)/2$ and $(b_n - a_n)/2$ were obtained by numerical integration of equations (34) and are shown in Fig. 12 and 13 for $\alpha = 0.7$ and 0.3 respectively. Here, as in the degenerate case, energy supplied by the pump does not produce exponential gain but rather produces a wave whose harmonic content becomes richer as it propagates along the transmission line. Again it is noticed that the amplitudes of the different side bands are higher, the smaller the value of α. This bears some similarity to the results shown in Fig. 5 and 6.

Bibliography

[1] *Tien, P. K.* and *H. Suhl:* A Traveling-Wave Ferromagnetic Amplifier. Proc. IRE Vol. 46(1958), No. 4, p. 700...706.

[2] *Tien, P. K.:* Parametric Amplification and Frequency Mixing in Propagating Circuits. J. appl. Phys. Vol. 29(1958), No. 9, p. 1347...1357.

[3] *Roe, G. M.* and *M. R. Boyd:* Parametric Energy Conversion in Distributed Systems. Proc. IRE Vol. 47(1959), No. 7, p. 1213 ...1218.

[4] *Louisell, W. H.* and *C. F. Quate:* Parametric Amplification of Space Charge Waves. Proc. IRE Vol. 46(1958), No. 4, p. 707...716.

[5] *Bridges, T. J.:* A Parametric Electron Beam Amplifier. Proc. IRE Vol. 46(1958), No. 2, p. 494...495.

[6] *Cullen, A. L.:* A Traveling-Wave Parametric Amplifier. Nature (London), Vol. 181(1958), No. 4605, p. 332.

[7] *Uspensky, T. V.:* Theory of Equations. New York: McGraw-Hill. 1948. p. 121.

Author's address:

Dr. *A. Dayem,* Bell Telephone Laboratories Inc., Murray Hill, N. J. (USA).

Theoretische Betrachtungen über den Einsatz eines parametrischen Verstärkers bei Radio-Teleskopen

Von *W. Druey,* Winterthur, und *H. Rickenbach,* Zürich

621.375.9.029.6 : 523.164

1. Verfahren für die Ermittlung der von einem schwarzen Strahler herrührenden Strahlungsintensität

Definition einer äquivalenten Antennentemperatur

Eine Antenne mit der Absorptionsfläche A und dem Wirkungsgrad η gibt bei Ausrichtung auf einen punktförmigen, unendlich weit entfernten schwarzen Strahler innerhalb eines relativ schmalen Frequenzbandes B an einen angepassten Verbraucher die Nutzleistung P_N ab:

$$P_N = \eta A B S'$$

S' Strahlungsintensität pro Hz Bandbreite

Ein anstelle der Antenne eingesetzter Widerstand R_A würde bei Anpassung die Rauschleistung P_R:

$$P_R = k T B$$

abgeben. Damit $P_R = P_N$ wird, muss der Widerstand R_A die Temperatur

$$T_A = \frac{\eta A S'}{k}$$

besitzen. T_A wird im folgenden die äquivalente Antennentemperatur oder kurz Antennentemperatur genannt. Sie ist ein Mass für die empfangene Strahlungsleistung.

Die von der Antenne abgegebene Nutz-Rauschleistung wird durch die Zuleitung zur Meßstelle um den Faktor a verringert, und die Zuleitung steuert entsprechend ihrer Temperatur T_L und dem Leistungsabschwächungsfaktor a ein zusätzliches Rauschen bei, so dass die an der Meßstelle auftretende Rauschleistung einer Temperatur T_A' entspricht. T_A' berechnet sich zu:

$$T_A' = a T_A + (1 - a) T_L$$

Differenzmessverfahren nach Dicke

Beim Differenzmessverfahren nach *Dicke* wird, wie Fig. 1 zeigt, der Empfängereingang periodisch zwischen Antennenzuleitung und einer Rauschquelle bekannter Leistung umgetastet, so dass am Ausgang des Zwischenfrequenzverstärkers ein rechteckförmig moduliertes Rauschen auftritt. Beträgt die Temperatur der durch einen Widerstand gebildeten Rauschquelle T_K und kommt durch den Empfänger eine der Temperatur T_E entsprechende Rauschleistung hinzu, so ändert die Rauschleistung am ZF-Ausgang zwischen den Werten

$$P_A = k [T_A' + T_E] B \cdot g_E \qquad (1)$$

und

$$P_K = k [T_K + T_E] B \cdot g_E \qquad (2)$$

g_E ist der Leistungsgewinnfaktor und B die Bandbreite des Empfängerhochfrequenzteiles. T_E ist die Temperatur, welche ein am Eingang des Empfängers befindlicher angepasster Widerstand besitzen müsste, um die im Empfänger entstehende Rauschleistung zu simulieren.

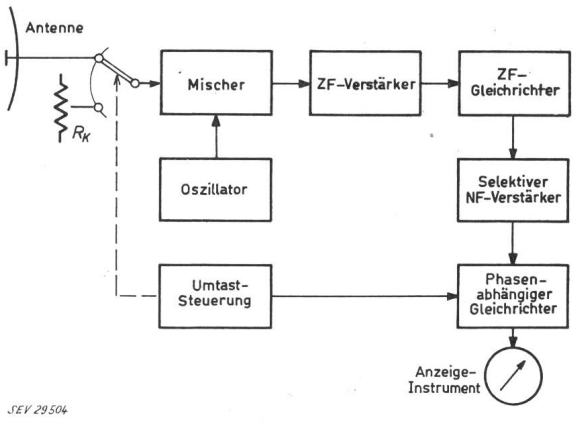

Fig. 1

Differenzmessverfahren nach Dicke

R_K Rauschquelle, z. B. Kohleschichtwiderstand

Das modulierte Rauschen wird mittels eines linearen Gleichrichters gleichgerichtet. Die entstehende «Gleich»-Spannung ändert periodisch zwischen Werten, die $\sqrt{P_A}$ und $\sqrt{P_K}$ proportional sind. Dem nachfolgenden Niederfrequenzteil wird somit eine Rechteckspannung geliefert, deren Amplitude proportional

$$\sqrt{T_A' + T_E} - \sqrt{T_K + T_E} \qquad (3)$$

ist. Mittels eines NF-Bandfilters wird aus der Rechteckspannung die Komponente mit der Grundfrequenz herausgesiebt. Ein Endverstärker führt das nun sinusförmige Signal einem phasenabhängigen Gleichrichter zu, so dass am Ausgang der Empfangsanlage eine Gleichspannung entsteht, welche für $T_A' > T_K$ positiv und für $T_A' < T_K$ negativ ist.

2. Problemstellung

Die Strahlungsintensitäten, welche noch gemessen werden sollen, entsprechen vielfach äquivalenten Antennentemperaturen von nur einigen °K. Demgegenüber liegt die Rauschtemperatur eines Empfängers mit Mischstufe am Eingang bei etwa $T_E = 1300$ °K.

Der Einfluss dieses hohen Eigenrauschens wird zwar durch die Anwendung des Differenzverfahrens erheblich